PCCP

Accepted Manuscript

ROYAL SOCIETY OF CHEMISTRY

www.rsc.org/pccp

Journal Name

COMMUNICATION

Highly selective uptake of carbon dioxide on the zeolite |$Na_{10.2}KCs_{0.8}$|-LTA – a possible sorbent for biogas upgrading

Received 00th January 20xx,
Accepted 00th January 20xx

DOI: 10.1039/x0xx00000x

www.rsc.org/

Ocean Cheung[a,b], Dariusz Wardecki[a], Zoltán Bacsik[a], Petr Vasiliev[c], Lynne B. McCusker[a,d] and Niklas Hedin[a*]

The |$Na_{10.2}KCs_{0.8}|_8[Al_{12}Si_{12}O_{48}]_8$($Fm\bar{3}c$)-LTA zeolite adsorbs CO_2-over-CH_4 with a high selectivity (over 1500). The uptake of carbon dioxide is also high (3.31 mmol/g, 293K, 101 kPa). This form of zeolite A is a very promising adsorbent for applications such as biogas upgrading, where keeping the adsorption of methane to a minimum is crucial.

In the last few decades, scientists and engineers have put a vast amount of effort into controlling the levels of greenhouse gas emission (GHG) through different means. Replacing some of the fossil fuel used in motor vehicles with upgraded biogas (called biomethane) is arguably an effective way of mitigating GHG emissions. This renewable transport fuel also seems to display the lowest emissions.[1]

Biomethane is typically produced from raw biogas through the anaerobic digestion (AD) of man-made waste products (and sometimes co-digestion with certain crops).[2] AD biogas needs to be purified to remove sulphur containing compounds, CO_2, siloxane and water. The content of CO_2 in biogas can be up to 50%, depending on the production method.[3] For fuel application, biogas usually needs to contain at least 95% methane in order to be compatible with compressed natural gas. Hence, the removal of CO_2 from biogas is essential. Today, biogas upgrading is done by water scrubbing,[4] amine-scrubbing,[5] polyethylene glycol absorption,[6] membrane separation,[7] cryogenic separation[8] or pressure swing adsorption (PSA).[9, 10] These methods have different advantages and disadvantages.[11] One advantage of the swing adsorption methods is that they can be downscaled to process small flows. This type of small scale upgrading is of great interest as it could allow larger quantities of biogas (than is possible today) to be produced in a cost effective way.

In swing adsorption processes, the dried AD gas is passed through adsorbent beds in a cyclic pattern, and the adsorbent selectively adsorbs CO_2, giving a stream of purified CH_4 at the end of the column(s). The properties of the adsorbent are therefore crucial to the process. The key factors are the CO_2 capacity[12], the CO_2 selectivity over CH_4[13] and the mechanical stability and the cost.[14] High CO_2 selectivity is especially important, as the co-adsorption of CH_4 can induce a "methane slip" that can lead to additional GHG emissions.[15] Therefore, methane slip has to be kept to a minimum either by adsorbent/process design or by catalytic burning.

Carbon molecular sieves are currently being used in commercialised PSA processes for biogas upgrading. However, their relatively low capacities for CO_2 imply that there is room for the development of alternative adsorbents. Many types of adsorbents, including zeolites[16, 17], metal organic frameworks [18], mesoporous materials[19] and clays[20] have been tested. Zeolites with small pore apertures can separate small molecules not only by their adsorption affinities, but also by kinetic or molecular sieving effects.[21-23] Certain zeolites with 8-ring (a ring consisting of 8 Si or Al and 8 O atoms in a zeolite framework) pores have pore openings similar to the kinetic dimensions of the gases of interest (CO_2 – 3.3Å, CH_4 – 3.8 Å).[24, 25] These zeolites appear to be especially well suited to deliver high selectivity for CO_2-over-CH_4. In some cases, it is possible to tune the differential diffusion rates of CO_2 and CH_4 (or N_2) by adjusting the composition of the zeolite.[26-28] The CO_2-over-C_2H_2 separation properties of ion-exchanged zeolite A (framework type **LTA**) was studied previously by Bülow et al.[29] They observed that zeolite A containing a mixture of sodium and potassium extra-framework cations could separate CO_2 from C_2H_2 very efficiently, and we recently demonstrated a similarly high selectivity for CO_2-over-CH_4.[30] Typically, there are three different sites in zeolite A for monovalent atomic (metal)

[a] Department of Materials and Environmental Chemistry and Berzelii Center EXSELENT on Porous Materials, Stockholm University, SE-106 91 Stockholm, Sweden. E-mail: niklas.hedin@mmk.su.se
[b] Nanotechnology and Functional Materials, Department of Engineering Sciences, Uppsala University, SE-751 21 Uppsala, Sweden
[c] NeoZeo AB, Villa Bellona, Universitetsvägen 10A, SE-106 91 Stockholm, Sweden.
[d] Laboratory of Crystallography,ETH Zürich, Wolfgang-Pauli-Strasse 10, CH-8093 Zürich, Switzerland.

† Footnotes relating to the title and/or authors should appear here.
Electronic Supplementary Information (ESI) available:. See
DOI: 10.1039/x0xx00000x

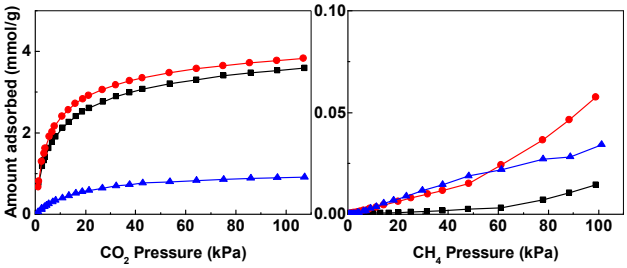

Figure 1: CO_2 (a) and CH_4 (b) adsorption isotherms of (red, ●)|$Na_{10}K_2$|-**LTA**, (blue, ▲) |$Na_{10}Cs_2$|-**LTA** and (black, ■) |$Na_{10.2}KCs_{0.8}$|-**LTA**.

cations. In the as-synthesised sodium-ion (Na^+) form, three Na^+ ions are located in 8-rings, eight in 6-rings and one near 4-rings. The resulting cation distribution gives a total of 12 Na^+ ions per **LTA** unit cell.[26] The cations in the 8-ring are of most interest in this study. The 8-rings allow the percolation of CO_2 and CH_4, while the 6- and 4-rings, because of their small apertures, do not. The percolation of the gas molecules through the 8-rings depends on which cation is occupying the site. Due to its small ionic radius, Na^+ prefers to sit off-centred of the 8-ring, so that it can make better contacts (albeit only on one side) with the negatively charged framework O atoms. As a result, Na^+ does not obstruct the diffusion of CO_2 or CH_4 through the 8-ring. K^+ and Cs^+, on the other hand, are both larger than Na^+. These large cations tend to occupy the centre of the 8-rings, and therefore obstruct the diffusion of CO_2 and CH_4. As CH_4 is larger than CO_2, the percolation of CH_4 is hindered by K^+ and Cs^+ to a larger extent than is CO_2. As previous studies have shown that both K^+ and Cs^+ ions exchange with the Na^+ ions located in the 8-ring sites first, [26, 31, 32] it is possible to control the ion-exchange process to tune the access to the pores of zeolite A to optimise the separation of CO_2 from CH_4.

The unit cell of zeolite |$Na_{10.2}KCs_{0.8}$|$_8$[$Al_{12}Si_{12}O_{48}$]$_8$($Fm\bar{3}c$)-**LTA** is eight times larger than that of the **LTA**-type framework (see formula above), as the latter does not distinguish between Si and Al atoms (tetrahedrally coordinated or T atoms) in the framework and assumes the highest possible symmetry. In the following discussion, the Si/Al ordering is not relevant. Therefore, we will use the smaller **LTA** unit cell (one *lta* or α cavity and one *sod* or β cage) for convenience.

A series of K^+ and Cs^+ ion-exchanged samples were prepared and tested (Table 1). In the K^+-exchanged samples, the uptake of CO_2 was found to be higher than that of CH_4 (Figure 1). The discrimination increased with the extent of K^+ exchange (from one ion per unit cell to two). For |$Na_{10}K_2$|-**LTA**, the estimated CO_2-over-CH_4 selectivity was ~230 for a CO_2/CH_4 mixture similar to raw biogas (for comparison, the selectivity of non-ion-exchanged |Na_{12}|-**LTA** was ~9). In |$Na_{10}K_2$|-**LTA**, two of the three 8-ring windows were occupied by K^+ and one by Na^+. With this configuration, the uptake of CH_4 decreased significantly but the CO_2 uptake remained high. It appeared that the K^+ ions hindered the percolation of CH_4, possibly because the energy barrier for diffusion through a K^+ occupied 8-ring window was high. Similar results were observed in our

Table 1. Cation compositions of the zeolite A samples, their CO_2 and CH_4 capacities (50 kPa, 293K) and their 8-ring cation occupancies

Cation compositions LTA	nCO_2 mmol/g	nCH_4 mmol/g	Select-ivity*	Fraction in 8-rings (%)		
				Na^+	K^+	Cs^+
|Na_{12}|	4.1	0.45	9	100	0	0
|$Na_{11}K$|	3.9	0.4	10	67	33	0
|$Na_{10}K_2$|	3.5	0.015	230	33	67	0
|$Na_{11}Cs$|	2.8	0.096	29	67	0	33
|$Na_{10}Cs_2$|	0.78	0.019	41	33	0	67
|$Na_{10.2}KCs_{0.8}$|	3.2	0.002	>1500	40	33	27
|$Na_{10.6}K_{0.6}Cs_{0.8}$|	3.5	0.11	32	53	20	27
|$Na_{10.6}K_{0.8}Cs_{0.6}$|	3.0	0.19	16	53	27	20
|$Na_{10.9}K_{0.6}Cs_{0.5}$|	3.4	0.31	11	63	20	17

*While the CO_2-over-CH_4 selectivity can be measured for a binary mixture by adsorption measurements or via breakthrough measurements, it can also be estimated from single component adsorption experiments. We estimated the selectivity for the adsorbents using this equilibrium based equation $s = (q_{CO2}/q_{CH4})/(p_{CO2}/p_{CH4})$, where q is the uptake of the gas at its partial pressure p, in the hypothetical mixture.

previous study on the adsorption of CO_2-over-N_2,[26, 33] where the uptake of N_2 dropped to almost zero. Mace et al.[34] showed that the energy barrier for the diffusion of CO_2 was lower than that of N_2 on zeolite |$Na_{10}K_2$|-**LTA**.

The high selectivity of the |$Na_{10}K_2$|-**LTA** sample could be improved further by replacing one of the K^+ ions with Cs^+ to form |$Na_{10.2}KCs_{0.8}$|-**LTA**. With this cation composition, the selectivity for CO_2 increased to >1500 whilst retaining a high uptake of CO_2 (~3.2 mmol/g, 293K, 50 kPa) (Note the very low methane uptake for these zeolites, hence the relative numerical error could be large. Considering this, the selectivity could conservatively be said to be > 500).

Even though the selectivity was only estimated using an equilibrium theory, the very high number indicated that this specific composition of zeolite A performs well in blocking the uptake of CH_4 without affecting that of CO_2. For the dual cation zeolites |$Na_{10}K_2$|-**LTA** and |$Na_{10}Cs_2$|-**LTA**, percolation theories also estimated that blockage of CH_4 occurred when the occupancy of the 8-ring (by K^+ and Cs^+) was 67%.[35] For the |$Na_{10}Cs_2$|-**LTA**, the Cs^+ cations in the 8-rings blocked the uptake of CH_4 and also the uptake of CO_2 to a large extent.

For the Cs^+-exchanged sample |$Na_{11}Cs$|-**LTA**, with Cs^+ ions occupying just one of the three 8-ring sites, the uptake of CO_2 was found to be significantly lower than for |$Na_{11}K$|-**LTA** (2.8 mmol/g vs. 3.9 mmol/g). With two Cs^+ ions per unit cell, the CO_2 uptake was reduced even further to just 0.78 mmol/g. Interestingly, for the mixed cation zeolite |$Na_{10.2}KCs_{0.8}$|-**LTA**, the CO_2 uptake was much higher (3.2 mmol/g). This difference in the CO_2 uptake could be related to the lower amount of Cs^+ in |$Na_{10.2}KCs_{0.8}$|-**LTA** than in |$Na_{11}Cs$|-**LTA** (Table 1).

In an attempt to better understand the reason for the percolation of CO_2 but not CH_4 in the |$Na_{10}K_2$|-**LTA** and |$Na_{10.2}KCs_{0.8}$|-**LTA** samples, we studied the crystal structure of a dehydrated version of the latter using high-resolution X-ray powder diffraction data. All diffraction peaks could be indexed in the cubic space group $Fm\bar{3}c$ with a = 24.5746(1) Å.

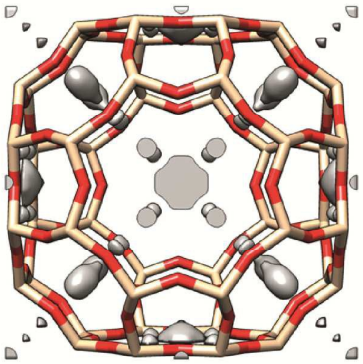

Figure 2: Difference electron density map generated for dehydrated |Na10.2KCs0.8|-LTA using just the framework atoms for the structural model.

As mentioned earlier, this unit cell took into account the strict alternation of Al and Si in the framework structure, so its volume is eight times larger than that of the framework type **LTA**. Rietveld refinement was initiated using the atomic parameters from the known crystal structure of **|Na_{12}|-LTA**.[36] In order to locate the non-framework cation sites, a difference electron density (or Fourier) map, in which only the framework atoms were included in the structural model, was calculated (Figure 2). The grey clouds in Figure 2 represent the electron density related to the positions of the non-framework cations. The map shows a significant peak near the centre of the 6-rings and a less well-defined peak in the 8-ring. Liu et al.[26] showed previously that for K^+-exchanged zeolite A with low K^+ concentrations, the site in the 6-ring remains occupied by Na^+. We therefore, assumed that this site was occupied only by Na^+ in our case and denoted it as Na(1). Taking into account the cation positions found in the fully exchanged zeolites **|Na_{12}|-LTA**[36], **|K_{12}|-LTA**[37] and in the zeolite **|Na_5Cs_7|-LTA**,[32] we interpreted the peak in the 8-ring as a superposition of three cation positions. In the zeolite **|Na_5Cs_7|-LTA**[32] the Cs^+ position was found to be in the centre of the 8-ring (site Cs(1)). However, our Fourier maps showed a second peak, shifted slightly off the mirror plane of the ring, that could also be assigned as a Cs^+ position (Cs(2)). The sum of the occupancies of these two sites gave 0.88(3) Cs^+ per a small unit cell, which was close to the chemical composition found by elemental analysis. We compared these results with the occupancies obtained for two other compositions i.e. **|$Na_{10.6}K_{0.8}Cs_{0.8}$|-LTA** and **|$Na_{10.6}K_{0.8}Cs_{0.6}$|-LTA**. The number of Cs^+ ions found per small unit cell was 0.88(3) and 0.56(2), respectively. The trend shows that these positions were indeed occupied by Cs^+ ions. A third position that was off-centre but on the mirror plane of the 8-ring can be interpreted as a K^+ position K(1). Four smaller clouds, further from the centre, were identified as Na^+ ions (Na(2)). According to Pluth et al. [36], there is another sodium position Na(3) in the α-cage opposite a 4-ring in **|Na_{12}|-LTA**, and this was also found to be present in our Fourier maps. A difference electron density map calculated using this model with the all the cations included showed a small peak on the 3 fold axis inside the α-cage that can be interpreted as residual water coordinated to Na^+ ions. Another water position was

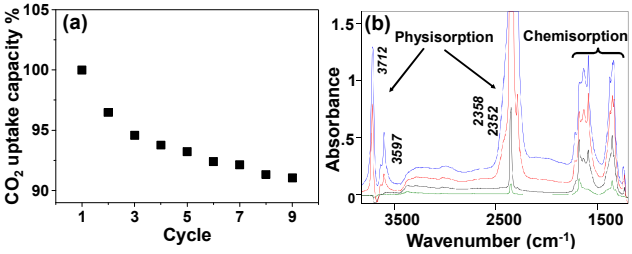

Figure 3: (a) Cyclic CO_2 uptake of **|$Na_{10.2}KCs_{0.8}$|-LTA** at 101 kPa and 293K. Regeneration of the zeolite in between cycles was done using dynamic vacuum (1×10^{-4} Pa) for 120 minutes at room temperature. In order to remove all chemisorbed CO_2, a heat treatment would have been required. (b) FTIR spectra of CO_2 adsorbed on **|$Na_{10.2}KCs_{0.8}$|-LTA**, adsorption branch at CO_2 pressures of 0.013 kPa, 0.040 kPa, 1.3 kPa and 13.3 kPa (bottom to top)

also indicated by a weak peak in the β-cage. Refinement of the diffraction data using a model including the cation and water positions presented above, gave a total of 12 cations and ~4 water molecules per small unit cell and R-values of about 6.6%. However, in all samples, the numbers of the K^+ and Na^+ ions in the 8-ring were larger than the values expected from the ICP measurements. The discrepancy could be explained by the presence of additional water molecules, which were not taken into account in the model. Figure S2 in the supporting material shows that the number of Na^+ ions in the 8-ring found in the refinement of **|Na_{12}|-LTA,** strongly depended upon the level of dehydration. The final values of the refined parameters for all samples are given in Tables S1-5.

The kinetics of adsorption of CO_2 for an adsorbent are very important for many applications, and the uptake of CO_2 on the highly selective zeolite **|$Na_{10.2}KCs_{0.8}$|-LTA** was found to be moderately fast. *In situ* infrared (IR) spectroscopy was used to monitor the development of the $\upsilon_1 + \upsilon_3$ combination band (3597 cm^{-1}) as the **|$Na_{10.2}KCs_{0.8}$|-LTA** sample was subjected to CO_2 at 13.3 kPa. These measurements showed that around 90% of the physisorbed CO_2 was adsorbed within ~ 180s of the exposure to CO_2.

The capacity of **|$Na_{10.2}KCs_{0.8}$|-LTA** to adsorb CO_2 decreased somewhat with successive cycles (Figure 3a). Around 3.5 % of the uptake capacity was lost after the first cycle, which was performed with a freshly prepared, vacuum- and heat-treated sample. Between the second and the third cycle, another ~ 2% was lost, and then less than 0.5 % was lost for each of the subsequent cycles. After nine cycles, the CO_2 uptake capacity was still 91 % of the original with about ~3.0 mmol/g of CO_2 at 293K and 101 kPa. The drop in the CO_2 capacity was related primarily to the chemisorption of CO_2, which occurred relatively slowly. The degree of chemisorption was consistent with that observed for different variants of zeolite A (typically up to 10% of the total adsorption).[33]

In situ infrared spectroscopy revealed, as expected, that CO_2 adsorbed on **|$Na_{10.2}KCs_{0.8}$|-LTA** mainly via physisorption. The differential IR spectra for CO_2 sorption in Figure 3b show numerous bands of physisorbed CO_2. The main band (around 2350 cm^{-1}) was assigned to the asymmetric stretching, υ_3. Within this main band, two different υ_3 bands were actually observed (at frequencies of 2352 and 2358 cm^{-1}). The two bands indicated that there were two different physisorption sites for CO_2 at very low pressures. Chemisorption of CO_2

(carbonate or carbonate like species) could be characterised with IR bands in the region of 1400 to 1750 cm^{-1}. Upon the removal of CO_2 by vacuum, the majority of the physisorbed CO_2 bands disappear (Figure S9). A small portion of the physisorbed CO_2 remains trapped inside the zeolite even at conditions of high dynamic vacuum (1 x 10^{-4} Pa, 303K), but could be removed easily by gentle heating to 343K. The chemisorbed CO_2 bands only disappeared when the material was regenerated by heating under vacuum at 523K.

Conclusions

In this study, we have performed a careful ion exchange of zeolite A (**|Na_{12}|-LTA)** to obtain different cation compositions in the Na-K, Na-Cs and Na-K-Cs systems. **|$Na_{10.2}KCs_{0.8}$|-LTA** shows very promising CO_2-over-CH_4 separation properties. The selectivity of this zeolite reached over 1500 (1 bar, 293K 50:50 CO_2:CH_4). Rietveld refinement shows that both K^+ and Cs^+ occupy 8-ring sites. These ions obstruct the percolation of CH_4 through the zeolite, while the CO_2 molecules could pass with a temporary displacement of the cation. The location of these large cations enhanced the CO_2 selectivity of the adsorbent without notably comprising its capacity. **|$Na_{10.2}KCs_{0.8}$|-LTA**, with its attractive CO_2-over-CH_4 separation properties and reasonably moderate kinetics for the adsorption of CO_2, is a potential adsorbent for upgrading biogas with a minimal CH_4 slip. The natural continuation of this adsorbent development process will be the optimisation of the adsorption kinetics.

Acknowledgements

Supported by the Swedish Research Council (VR), the Swedish Governmental Agency for Innovation Systems (VINNOVA) through the Berzelii Center EXSELENT, the Swedish Energy Agency and the Röntgen-Ångström Cluster MATsynCELL.

Notes and references

1. R. Edwards, J. Larivé and W. Weindorf, *Well-to-wheels analysis of future automotive fuels and powertrains in the European context*, Institute of Energy and Transport, European Commission (Luxembourg), 2013.
2. L. Hamelin, I. Naroznova and H. Wenzel, *Appl. Energy*, 2014, **114**, 774-782.
3. G. J. Farquhar and F. A. Rovers, *Water, Air, Soil Pollut.*, 1973, **2**, 483-495.
4. S. S. Kapdi, V. K. Vijay, S. K. Rajesh and R. Prasad, *Renewable Energy*, 2005, **30**, 1195-1202.
5. G. T. Rochelle, *Science*, 2009, **325**, 1652-1654.
6. R. A. Davis and O. C. Sandall, *AlChE J.*, 1993, **39**, 1135-1145.
7. S. Basu, A. L. Khan, A. Cano-Odena, C. Liu and I. F. J. Vankelecom, *Chem. Soc. Rev.*, 2010, **39**, 750-768.
8. M. J. Tuinier and M. van Sint Annaland, *Ind. Eng. Chem. Res.*, 2012, **51**, 5552-5558.
9. A. Alonso-Vicario, J. R. Ochoa-Gómez, S. Gil-Río, O. Gómez-Jiménez-Aberasturi, C. Ramírez-López, J. Torrecilla-Soria and A. Domínguez, *Microporous Mesoporous Mater.*, 2010, **134**, 100-107.
10. A. Arya, S. Divekar, R. Rawat, P. Gupta, M. O. Garg, S. Dasgupta, A. Nanoti, R. Singh, P. Xiao and P. A. Webley, *Ind. Eng. Chem. Res.*, 2015, **54**, 404-413.
11. E. Ryckebosch, M. Drouillon and H. Vervaeren, *Biomass. Bioenergy*, 2011, **35**, 1633-1645.
12. M. Mofarahi and F. Gholipour, *Microporous Mesoporous Mater.*, 2014, **200**, 1-10.
13. Y. S. Bae and R. Q. Snurr, *Angew. Chem., Int. Ed.*, 2011, **50**, 11586-11596.
14. M. T. Ho, G. W. Allinson and D. E. Wiley, *Ind. Eng. Chem. Res.*, 2008, **47**, 4883-4890.
15. M. Ravina and G. Genon, *J. Clean Prod.*, 2015, **102**, 115-126.
16. V. R. Choudhary and S. Mayadevi, *Langmuir*, 1996, **12**, 980-986.
17. T. Montanari, E. Finocchio, E. Salvatore, G. Garuti, A. Giordano, C. Pistarino and G. Busca, *Energy*, 2011, **36**, 314-319.
18. B. Li, H.-M. Wen, W. Zhou and B. Chen, *J. Phys. Chem. Lett.*, 2014, **5**, 3468-3479.
19. B. Yuan, X. Wu, Y. Chen, J. Huang, H. Luo and S. Deng, *Environ. Sci. Technol.*, 2013, **47**, 5474-5480.
20. M. s. L. Pinto, J. Pires and J. Rocha, *J. Phys. Chem. C*, 2008, **112**, 14394-14402.
21. D. M. Ruthven, *Adsorption*, 2001, **7**, 301-304.
22. H. Yucel and D. M. Ruthven, *J. Colloid Interface Sci.*, 1980, **74**, 186-195.
23. S. C. Reyes, V. V. Krishnan, G. J. DeMartin, J. H. Sinfelt, K. G. Strohmaier and J. G. Santiesteban, *U. S. Patent*, 2004.
24. R. C. Weast, *CRC Handbook of Chemistry and Physics*, 48 edn., CRC Press, 1967.
25. B. Poling, J. Prausnitz and J. O. Connell, *The Properties of Gases and Liquids*, Mcgraw-hill, 2000.
26. Q. Liu, A. Mace, Z. Bacsik, J. Sun, A. Laaksonen and N. Hedin, *Chem. Comm.*, 2010, **46**, 4502-4504.
27. A. Lauerer, T. Binder, C. Chmelik, E. Miersemann, J. Haase, D. M. Ruthven and J. Karger, *Nat Commun*, 2015, **6**.
28. T. Remy, E. Gobechiya, D. Danaci, S. A. Peter, P. Xiao, L. Van Tendeloo, S. Couck, J. Shang, C. E. A. Kirschhock, R. K. Singh, J. A. Martens, G. V. Baron, P. A. Webley and J. F. M. Denayer, *RSC Adv.*, 2014, **4**, 62511-62524.
29. *M. Bulow, C. J. Guo, D. Shen, F. R. Fitch, A. I. Shirley, A. I. L. Cava, S. B. Dougill and J. P. Brooks, United States Pat.,U. S. Patents*, US6024781 A, 2000.
30. Z. Bacsik, O. Cheung, P. Vasiliev and N. Hedin, *Appl. Energy*, 2016, **162**, 613-621.
31. N. H. Heo, C. Dejsupa and K. Seff, *J. Phys. Chem.*, 1987, **91**, 3943-3944.
32. T. B. Vance and K. Seff, *J. Phys. Chem.*, 1975, **79**, 2163-2167.
33. O. Cheung, Z. Bacsik, Q. Liu, A. Mace and N. Hedin, *Appl. Energy*, 2013, **112**, 1326-1336.
34. A. Mace, K. Laasonen and A. Laaksonen, *Phys. Chem. Chem. Phys.*, 2014, **16**, 166-172.
35. D. Keffer, A. V. McCormick and H. T. Davis, *J. Phys. Chem.*, 1996, **100**, 967-973.
36. J. J. Pluth and J. V. Smith, *J. Am. Chem. Soc.*, 1980, **102**, 4704-4708.
37. J. J. Pluth and J. V. Smith, *J. Phys. Chem.*, 1979, **83**, 741-749.

Zeolite |$Na_{10.2}KCs_{0.8}$|-LTA was found to be a promising adsorbent for applications such as biogas upgrading. The CO_2-over-CH_4 selectivity was very high (over 1500)